RSC Advances

ROYAL SOCIETY OF CHEMISTRY

www.rsc.org/advances

Cite this: DOI: 10.1039/c0xx00000x

www.rsc.org/xxxxxx

ARTICLE TYPE

Friction mechanism of zinc oxide films prepared by atomic layer deposition

Zhimin Chai,[a] Xinchun Lu,*[a] and Dannong He[b]

Received (in XXX, XXX) XthXXXXXXXXX 20XX, Accepted Xth XXXXXXXXX 20XX

DOI: 10.1039/b000000x

Friction and wear can make the normal operation of zinc oxide (ZnO) films in many devices impracticable. In this paper, the friction mechanism of ZnO films was studied. The ZnO films were prepared by atomic layer deposition (ALD) on a Si (111) substrate, and the crystal structure of the films was controlled by adjusting the substrate temperature. The surface morphology, microstructure and composition of the ZnO films were studied by a scanning probe microscopy (SPM), a transmissionelectron microscopy (TEM) and an Auger electron microscopy (AES), respectively. The friction coefficient of the ZnO films was measured by a ball-on-disk tester. The results show that the ZnO film deposited at 300 °C has lager crystal size than that deposited at 150 °C. In addition, the 300 °C deposited ZnO film consists of mainly (002)-textured nanocrystal, while the 150 °C deposited ZnO film consists of other orientational nanocrystal, such as (100) and (101)-textured nanocrystals. The friction coefficient of the ZnO films is ~0.1, much smaller than 0.6 of the Si (111) substrate. Low friction coefficient is attributed to plastic deformation induced nanocrystal structure to amorphous structure transformation. The 150 °C deposited ZnO film has smaller crystal size than the 300 °C deposited ZnO film, and thus deformation more easily and the friction coefficient is smaller.

Keywords: ZnO; atomic layer deposition; friction; amorphous structure

1. Introduction

Wurtzite type zinc oxide (ZnO), having a direct wide band gap of 3.37 eV, a large exciton binding energy of 60 meV, and excellent piezoelectric and transparent properties, has attracted much attention in optoelectronic applications. It is a promising material for making transparent high power electronics, UV light-emitters, piezoelectric transducers and solar cells.[1, 2] In some of these applications, moving or touching structures are inevitable. The relative motion of moving parts may induce wear of ZnO films used therein, and thus the performance of the device may be degraded. Therefore, it's of great significance to investigate the tribological behavior of the ZnO films for device applications.

Zabinski et al. have studied the tribological behavior of ZnO films prepared by pulsed layer deposition (PLD) at various test conditions,[3-6] and the results revealed that the friction coefficients of these films were in the range of 0.15~0.2, much smaller than that (ranging from 0.6 to 0.7) of bulk ZnO. Moreover, the wear life of these films was very long, over one million cycles. The improved tribological performance of the ZnO films had been attributed to their nanocrystalline character. In addition, the (002) textured grain structure of the ZnO films was also considered contributing to their improved tribological performance. In subsequent studies, Mohseni et al. introduced an Al_2O_3 underlayer to ZnO films to enhance their (002) texture, and demonstrated that ZnO films with the (002)-orientation exhibited a smaller friction coefficient than those films with nanocrystalline randomly orientation.[7, 8] However, our previous study revealed that ZnO films with (002)-orientation as well as (100) and (101)-orientations possessed a small friction coefficient.[9] Therefore, whether ZnO films with orientations other than (002)-orientation can reduce friction should be further studied.

ZnO films with different orientations can be deposited by an atomic layer deposition (ALD) technology.[10, 11] ALD is a modification of chemical vapor deposition (CVD) technology by which two precursors are pulsed into a reaction chamber alternately, and between the precursor cycles, the reaction chamber was purged with an inert gas. A key feature of ALD is self-limiting, which enables the growth of highly uniform and conformal films.[12, 13] Furthermore, the film thickness can be controlled at a monolayer level.

In this work, ZnO films were deposited on a Si (111) substrate by ALD at substrate temperatures of 150 °C and 300 °C. The crystal structure of the ZnO films was characterized by a transmission electron microscopy (TEM), and the friction coefficient of the ZnO films was measured by a ball-on-disk dry sliding tester. In order to make clear the mechanism of the improved tribological property of ZnO films, site selective TEM samples were prepared inside the wear track.

2. Experimental

2.1 Film preparation

ZnO films were grown on a Si (111) substrate using a SUNALE^{TM} R-series ALD UNIT (Picosun). The two precursors used were Diethylzinc (DEZ, purity >99.99%) and water.[14, 15] These two precursors were alternately injected into the reaction chamber using a high purity nitrogen (purity >99.999%) as a carrier gas. One complete ALD cycle consists of four steps: (1) pulse of DEZ precursor for 0.1 s, (2) purge the reaction chamber with the high purity nitrogen for 3 s, (3) pulse of water precursor for 0.1 s, and (4) purge the reaction chamber with the high purity nitrogen for 4 s. The desired ZnO films were obtained by repeating the ALD cycle for 500 times.

Prior to film deposition, the Si (111) substrate was ultrasonically cleaned in acetone, absolute alcohol and deionized water for 10 min, respectively, and then blow-dried with a purity nitrogen (purity >99.99%). During deposition, the base pressure of the reaction chamber was kept 600-700 Pa using a dry pump, and the temperature of the chamber was set at 150 °C and 300 °C to get ZnO films with different crystal structures.[16] In our previous study, we have demonstrated that all the ZnO films have (002) orientation (c-axis preferred orientation)[9] because the (002) plane is the most densely packed and thermodynamically favorable plane of ZnO.[17] However, the ZnO film deposited at 150 °C also has other orientations, such as (100) and (101)-orientations (a-axis preferred orientation).

2.2 Film characterization

The thickness of the ZnO films was measured by a null-ellipsometry (Multiskop, Optrel). The wavelength of the laser was 632.8 nm and the incidence angle was 70°. The obtained film thickness of ZnO films prepared at 150 °C and 300 °C were 103.9 ± 0.6 nm and 87.7 ± 0.5 nm, respectively. Surface morphology of the ZnO films was obtained by a NanoScope IIIA scanning probe microscopy (SPM, Veeco) in a tapping mode with a PPP-NCHR probe (NanoSensors, nominal spring constant 42 N/m and resonant frequency ~300 kHz).

The crystal structure of the ZnO films was analyzed by TEM (JEOL 2011) operated at a 200 kV accelerating voltage. For plan-view observation, a TEM specimen was prepared by mechanical polishing followed by Ar ions milling from the substrate side, and then the surface of ZnO film was slightly milled to remove the contamination. A cross-sectional TEM specimen was prepared by forming a sandwich with epoxy followed by mechanical polishing and then Ar ion milling.

The elemental concentration across the ZnO films was obtained by an Auger electron microscopy (AES, PHI-700) with a co-axial cylindrical mirror analyzer (CMA). The AES was operated at a pressure of $<3.9\times10^{-9}$ Torr. A 5 kV Ar ion beam was used to sputter the ZnO films. The incident angle was 30°, and the sputtering rate of a SiO_2 film (calibration specimen) was 4 nm/min.

2.3 Friction test

The friction coefficient of the ZnO films was measured by a ball-on-disk tester (UMT, Bruker) in the ambient air. The test was performed in a reciprocating sliding mode against a commercial Si_3N_4 ball of 3.969 mm diameter, ~15 nm Ra roughness and 310 GPa elastic modulus. The normal load was in the range of 0.25-2.5 N, which corresponded to initial maximum Hertzian contact stresses of 379.8-818.3 MPa. Before the friction test, the Si_3N_4 ball was cleaned by absolute alcohol. During the friction test, the reciprocating frequent was set as 0.5 Hz and sliding amplitude was set as 1 mm. Friction tests were run for 1800 cycles, and at least 5 tests were made for each sample.

After the friction test, the wear track was observed by an optical microcopy, and a scanning electron microscope (SEM, FEI Quanta 200 FEG) operating at 20 kV accelerating voltage. TEM samples were made in the wear track along the direction of sliding using a focused ion beam (FIB) equipped scanning electron microscope (Tescan, Lyra 3) to determine the friction mechanism. The element distribution on the TEM sample was studied by energy-dispersive X-ray spectroscopy (EDS).

3. Results and discussion

3.1 Film characterization

The surface morphology of the ZnO films was investigated by AFM. Figure 1 (a) and (b) show AFM images of the ZnO films deposited at 150 °C and 300 °C, respectively. It can be seen that a large amount of asperities cover the ZnO surface. An asperity is expected to be an individual crystalline grain, which will be demonstrated by planar TEM images below. The grains of the ZnO film deposited at 300 °C are uniform, while grains of ZnO film deposited at 150 °C aren't uniform, and with some large peaks. Due to these large peaks, the RMS roughness of the ZnO film deposited at 150 °C is 6.06 nm, much larger than 1.68 nm of the ZnO film deposited at 300 °C. Though the ZnO film deposited at 150 °C has large peak, the average grain size of the film is smaller than that of the ZnO film deposited at 300 °C. The grain size of the ZnO film deposited at 150 °C is in the range of 20-40 nm (apart from the large peaks), while the grain size of ZnO film deposited at 300 °C is in the range of 30-40 nm.

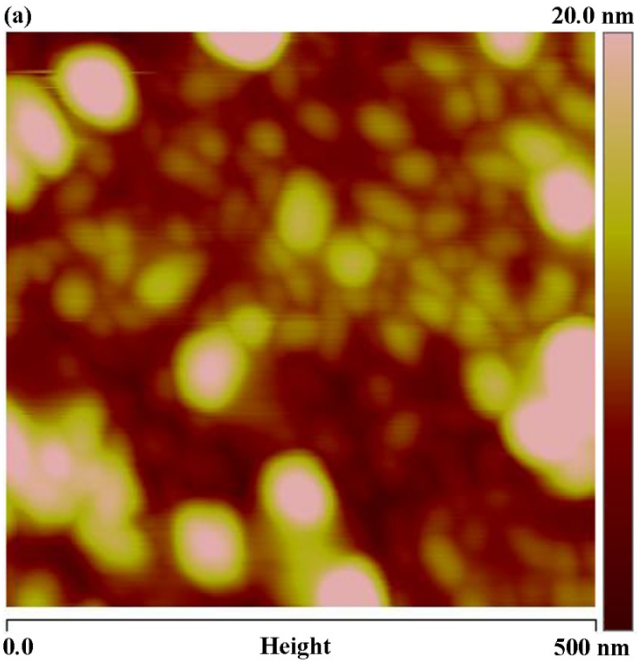

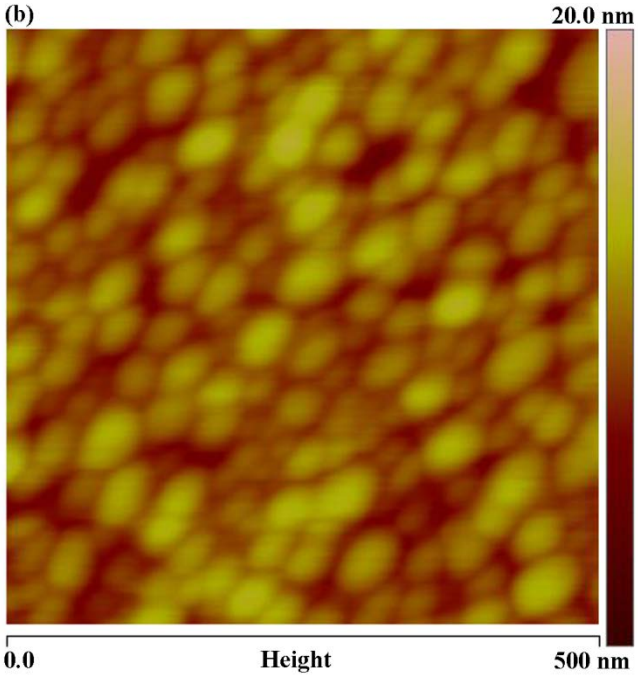

Figure 1. AFM images of the ZnO films deposited at 150 °C (a) and 300 °C (b), respectively.

Figure 2 (a) is a planar TEM image of the ZnO film deposited at 300 °C. It can be seen that the crystal size of the ZnO film deposited at 300 °C is uniform, in the range of 30-40 nm, which corresponds well with the grain size measured by AFM. Therefore, it can be concluded that each asperity in the AFM image is a nanocrystal.

High resolution TEM image of the nanocrystalline grain is shown in Figure 2 (b). The distances between lattice planes, indicated by 'A' and 'B' in the TEM image, are 2.775 and 2.736 nm, respectively. These values are close to 2.814 nm, which is the interplanar spacing of the (100) plane. Because the (100) plane is perpendicular to the (002) plane, it means that the c-axis (002) orientation is obtained for the ZnO film deposited at 300 °C, which are consistent with our previous study.[9]

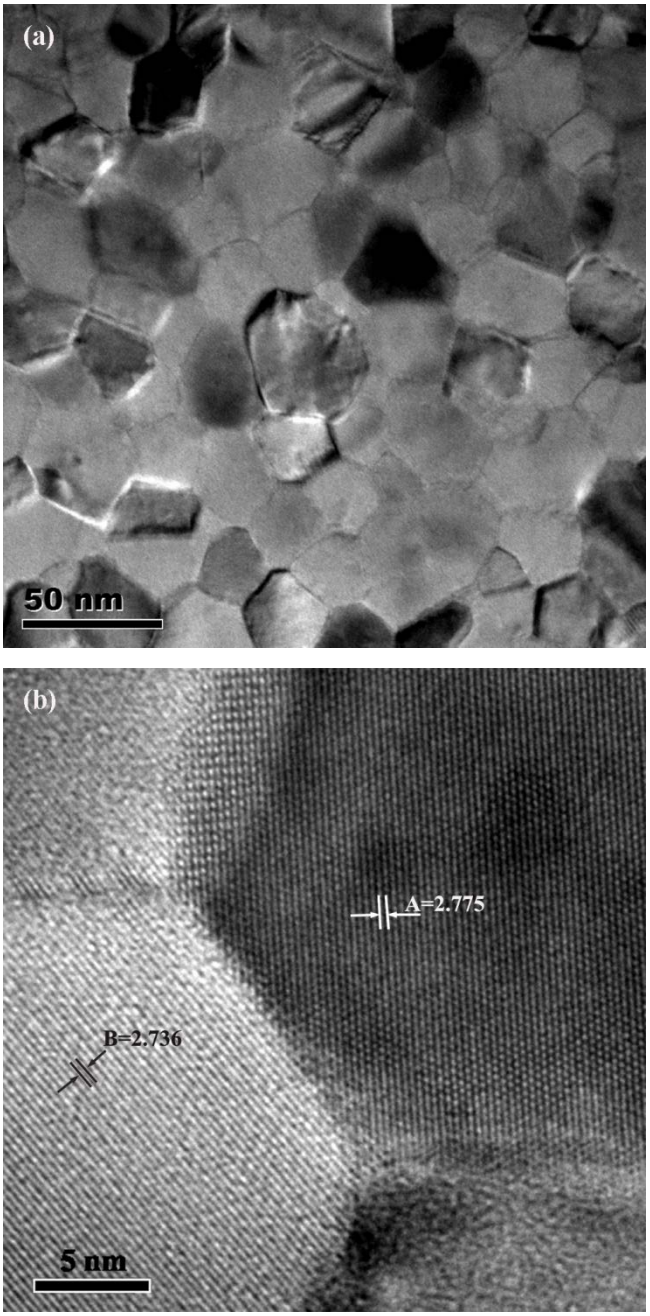

Figure 2. (a) Planar TEM image of the ZnO film deposited at 300 °C; (b) high resolution TEM image of the ZnO film deposited at 300 °C.

Figure 3 (a) and (b) are cross-sectional TEM images of the ZnO films deposited at 150 °C and 300 °C, respectively. The white arrow indicates the direction of the Si (111) substrate. Only one grain is visual in Figure 3 (b). The distance between lattice planes is 2.611, which is close to the interplanar spacing of the (002) plane, further demonstrating that ZnO film deposited at 300 °C has c-axis orientation. However, several grains can be seen in Figure 3 (a), and the grain boundaries can be seen clearly. The distances between lattice planes, indicated by 'A', 'B' and 'C' in the TEM image, are 2.467, 2.786 and 2.642 nm, which are the interplanar spacing of the (101), (100) and (002) planes, respectively. The result also demonstrates that ZnO film deposited at 150 °C has a-axis orientation other than c-axis

orientation.[9]

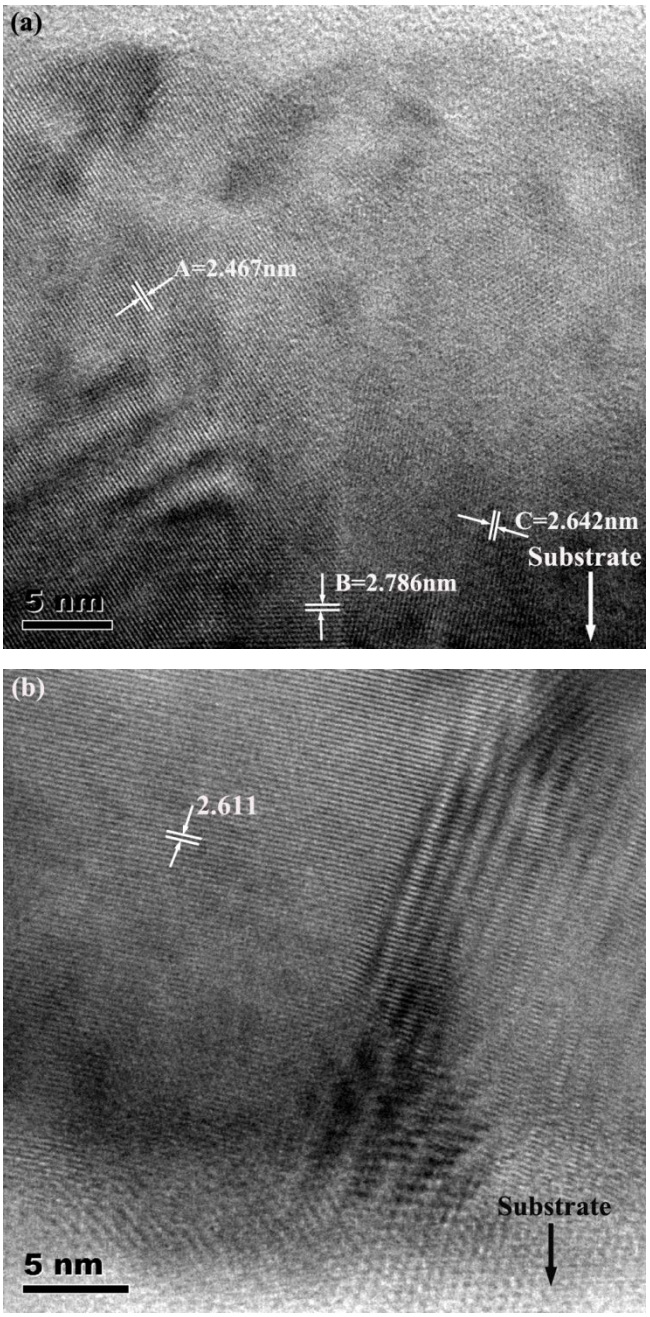

Figure 3. High resolution cross-sectional TEM images of the ZnO films deposited at 150 °C (a) and 300 °C (b), respectively.

AES was used to analyze the chemical composition of the ZnO films. Figure 4 (a) and (b) show the elemental depth profiles of the ZnO films deposited at 150 °C and 300 °C, respectively. Relative ratio of element content is shown in Table 1. Normalization was done by setting the content of Zn as 1. Both the ZnO films show an oxygen-deficient chemical composition, with an oxygen-to-zinc ratio of ~0.9. The oxygen-to-zinc ratio in our study is higher than that reported by Jeon et al.,[14] which is in the range of 0.75 to 0.97. The oxygen deficiency of the ZnO films may be due to the fact that DEZ and water precursors did not react adequately. DEZ precursor remains in the ZnO films,[18] which is demonstrated by the carbon composition in the ZnO films.

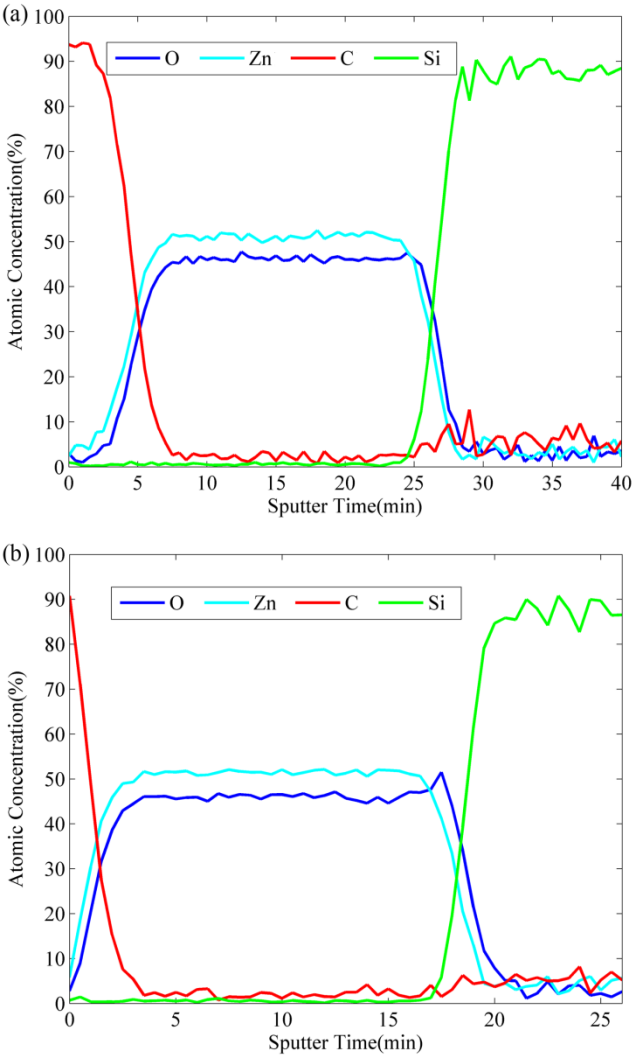

Figure 4. AES composition depth profiles of the ZnO films deposited at 150 °C (a) and 300 °C (b).

Table 1. Relative ratio of element content of ZnO films deposited at various temperatures.

Elements	Deposition temperature	
	150 °C	300 °C
Zn	1	1
O	0.90	0.89
C	0.042	0.042

3.2 Tribological behavior

The tribological behavior of the ZnO films was measured by the ball-on-disk tester. Figure 5 (a) shows the friction coefficient of the ZnO films deposited at 150 °C and 300 °C at the normal load of 0.5 N. In the initial run-in period, the friction coefficient is high, and then the friction coefficient tends to become stable. A similar run-in period has been reported by Prasad et al..[4] The reason for this run-in period will be discussed below. After 1800 cycles friction test, steady-state friction coefficients of 0.085 and 0.106 are reached for ZnO films deposited at 150 °C and 300 °C, respectively. Small friction coefficient of the ZnO films is attributed to their nanocrystalline characteristic. Because the

crystal size of ZnO film deposited at 150 °C is smaller than that of ZnO film deposited at 300 °C, the ZnO film deposited at 150 °C deforms more easily, and thus the friction coefficient is smaller.[9]

Figure 5 (b) shows the friction coefficient of the Si (111) substrate. Usually, a native oxide layer of ~1.5 nm exists on the surface of the Si (111) substrate.[19-21] The hardness of the SiO_2 layer (~2.0 GPa[22]) is much smaller than that of the Si (111) substrate (~11.5 GPa[21]), and thus the oxide layer can be sheared easily and the initial friction coefficientis small. When the native oxide layer is worn out, the friction coefficient increases. The steady-state friction coefficient of the Si (111) substrate is 0.59. Because ZnO films have a much smaller friction coefficient than that of the Si (111) substrate, they can be used as friction protective coating for Si material.

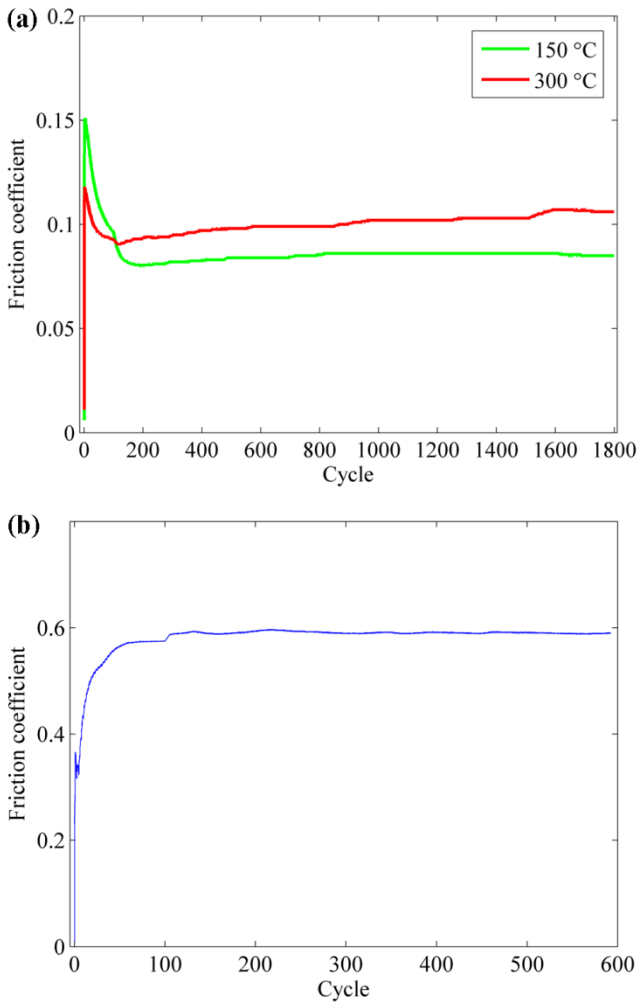

Figure 5. Friction coefficient traces of (a) the ZnO films deposited at 150 °C and 300 °C and (b) the Si (111) substrate at the normal load of 0.5 N.

Figure 6 shows the friction coefficient of ZnO films as a function of normal load. The result reveals an Amontonian friction behavior, that is, the friction coefficient does not change much with the variation of normal load. The average friction coefficients of the ZnO films deposited at 150 °C under various normal loads are smaller than those of the ZnO films deposited at 300 °C. However, there is an overlap between the friction coefficient values when the standard deviation is considered. Lower friction coefficient of the ZnO films deposited at 150 °C is likely attributed to their smaller crystal size.[9] As mentioned above, the ZnO films deposited at 150 °C have orientations other than (002) orientation, such as (101) and (100) orientations, which means that (002) orientation is not essential for low friction coefficient.

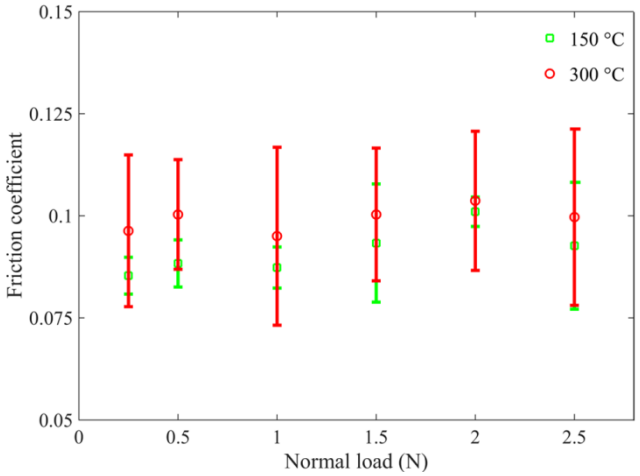

Figure 6. The friction coefficient of ZnO films deposited at 150 °C and 300 °C under various normal loads.

Figure 7 shows the optical microscopy image of the wear track for ZnO film deposited at 150 °C under normal load of 0.5 N. In most of the wear track area, the ZnO film is not worn out since the blue color marking the ZnO film can still be seen. While, in certain areas, the ZnO film is worn out. The maximum contact stress between the Si_3N_4 ball and the ZnO film at the normal load of 0.5 N is 478.5 MPa, much smaller than the hardness of the ZnO film.[9] That is why most of the ZnO film is not worn out. However, some local asperities exist on the Si_3N_4 ball. The contact stress between the Si_3N_4 ball and the ZnO film at the location of asperities is very large. When the contact stress is larger than the hardness of the ZnO film, the film will be worn out. This explains why the ZnO film at some local areas undergoes serve wear.

Figure 7. Optical microscopy image of the wear track for ZnO film deposited at 150 °C under normal load of 0.5 N.

Figure 8 (a) shows the SEM image of the wear track taken at the same area as that taken for optical microscopy image. Figure 8 (b) is a magnified image of the selected area in (a). From this

image, we can clearly see that the ZnO film is worn out locally.

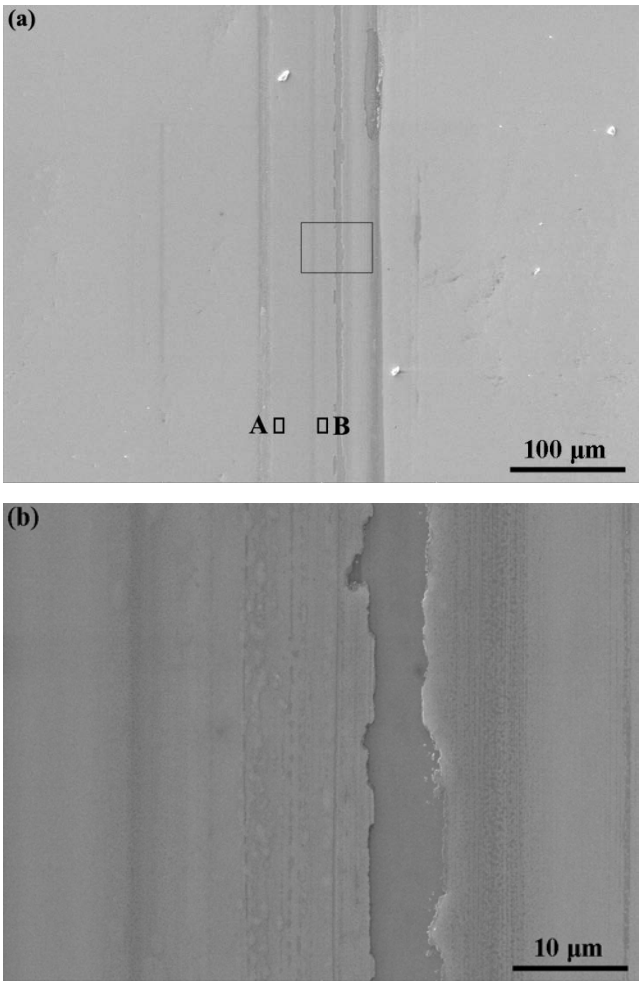

Figure 8. (a) SEM image of the wear track for ZnO film deposited at 150 °C under normal load of 0.5 N; (b) A magnified image of the selected area in (a).

In order to make clear the friction mechanism, FIB prepared cross-sectional TEM samples are studied inside the wear track. Figure 9 (a) shows the cross-sectional TEM image inside the center of the wear track taken at location B in Figure 8 (a). The image reveals that ZnO film only undergoes slight wear. The film thickness decreases from 103.9 nm to 95.0 nm. An amorphous layer of ~21.9 nm appears between the ZnO film and the protective Pt layer. The existence of this layer has been reported in a previous study.[23] They attributed this layer to be ZnO film which is transformed from nanocrystal structure to amorphous structure. The transformation process may be the continuous decreasing the grain size to amorphous structure. Because the amorphous layer can be sheared easily, the steady-state friction coefficient of the ZnO film is low. While at the initial period of friction test, the transformation process does not happen. The contact occurs between the Si_3N_4 ball and the nanocrystallineZnO film, and thus the friction coefficient is very large, which explains the run-in period mentioned above.

Figure 9 (b) shows the cross-sectional TEM image inside the wear track taken at location A in Figure 8 (a), and Figure 9 (c) is a magnified image of (b) which is taken at the interface of the ZnO film and the amorphous layer. It can be seen that the amorphous layer is also present. Selected area diffraction (SAD) pattern of this layer in Figure 9 (d) shows halo rings, which further demonstrates the amorphous structure of this layer. The thickness of the amorphous layer is ~129.6 nm, much larger than the thickness of the layer in Figure 9 (a). The difference between the thickness of amorphous layers is ascribed to the different stress states in the wear track. The contact stress between the Si_3N_4 ball and the ZnO film in the center of the wear track is larger than that in the side of the wear track.[24] Therefore, during the friction test, the amorphous ZnO layer formed in the center of the track is extruded to the side of the track, which explains why the thickness of the amorphous layer at the side of the wear track is larger.

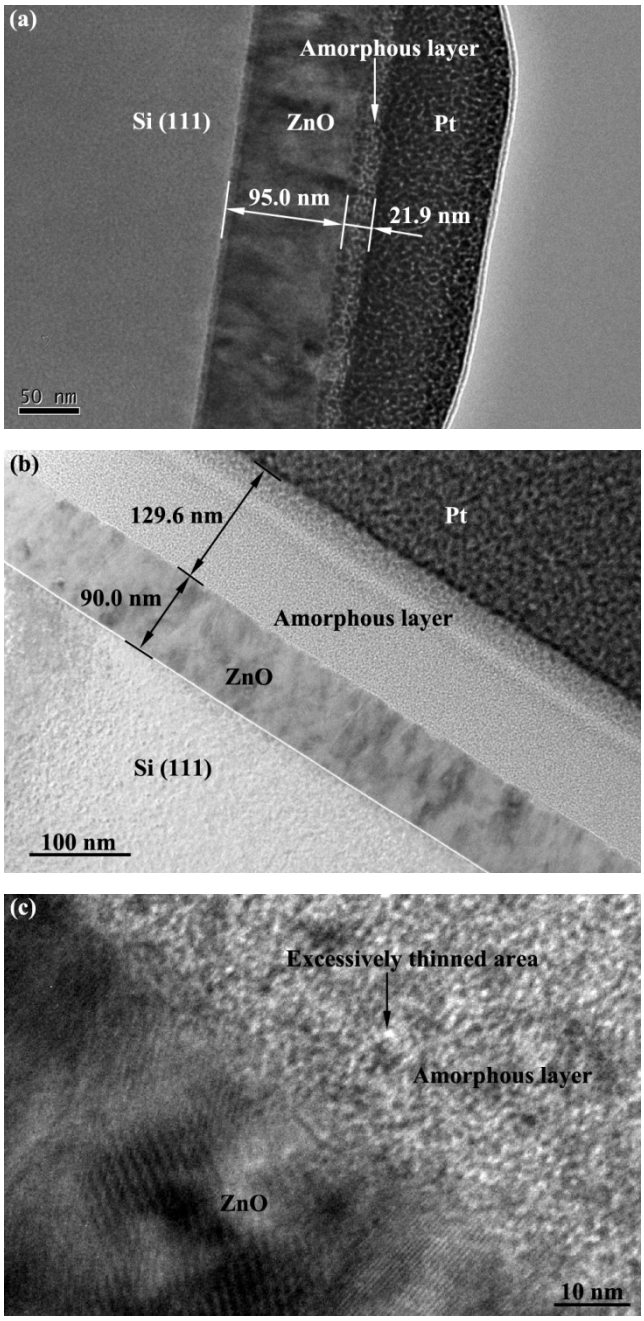

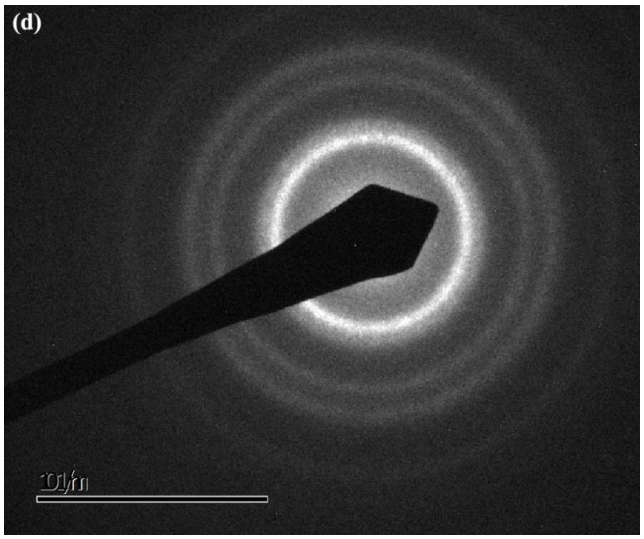

Figure 9. (a) Cross-sectional TEM image inside the center of the wear track taken at location B in Figure 8 (a); (b) Cross-sectional TEM image inside the wear track taken at location A in Figure 8 (a); (c) A magnified image of (b); (d) SAD pattern of the amorphous layer.

Figure 10 shows the cross-sectional TEM image and corresponding EDS element maps of the sample taken at the side of the wear track. The Pt layer, amorphous layer, ZnO layer and the Si (111) layer are layered obviously, and all the layers show sharp interfaces. The observation of ZnO layer demonstrates that ZnO film is not worn out during the friction test. It should be mentioned that the concentration of all the elements in the amorphous layer is low. This is likely due to that the amorphous layer is ultra-thin. The amorphous layer usually does not have strong mechanical strength. When preparing the TEM sample, the amorphous layer can be excessively thinned by high energy Ga ions, and some local areas can even be thinned through. In Figure 9 (c), it can be seen that excessive thinned area shows a micro-hole. Even if low concentration, Zn and O elements can be detected in the amorphous layer, which demonstrates that the amorphous layer is ZnO.

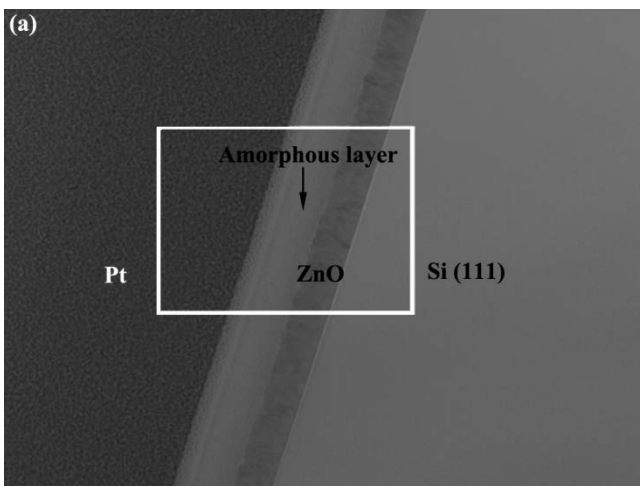

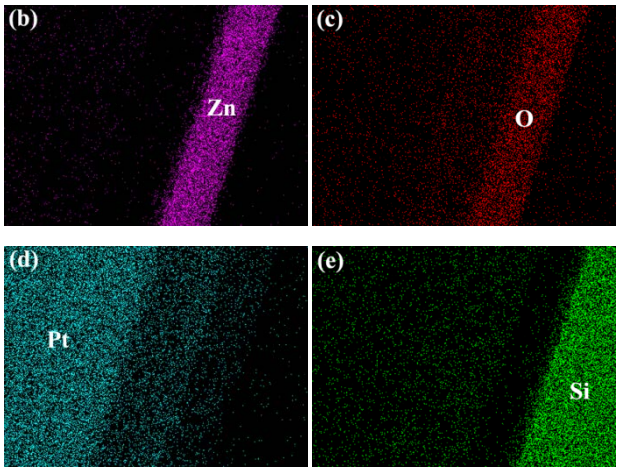

Figure 10. (a) Cross-sectional TEM image of the sample taken at the side of the wear track (location A in Figure 8 (a)); (b), (c), (d) and (e) are corresponding EDS element maps.

4. Conclusion

ZnO films with thickness of ~100 nm were prepared by ALD on the Si (111) substrate at the substrate temperature of 150 °C and 300 °C. The grain size of the ZnO film deposited at 300 °C is large and uniform (30-40 nm), while the grain size of the ZnO film deposited at 150 °C is not uniform (20-40 nm), with large peaks. Planar TEM results demonstrate that each grain in the AFM image is a nanocrystal. In the ZnO film deposited at 300 °C, c-axis orientated (002) plane parallel to the substrate is dominated, while at 150 °C other orientations, such as (100) and (101), are also observed. The friction test demonstrates that not only the 300 °C deposited ZnO film with c-axis preferred orientation shows a low friction coefficient, but also the 150 °C deposited ZnO film with a-axis orientation shows a low friction coefficient. The friction coefficient of 150 °C deposited ZnO film is smaller because of the smaller crystal size. TEM sample inside the wear track shows an amorphous layer. The amorphous layer has a low shear strength, which contributes to the low friction coefficient of ZnO films.

Acknowledgements

The authors greatly appreciate the financial support of the National Science Fund for Distinguished Young Scholars (50825501), the Science Fund for Creative Research Groups (51321092), the National Natural Science Foundation of China (51335005 and 91323302), and the National Science and Technology Major Project (2008ZX02104-001). Helpful discussions with Wen Jing are gratefully acknowledged.

Notes and references

[a] *The State Key Laboratory of Tribology, Tsinghua University, Beijing 100084, China. Telephone/Fax: +86 10 6279 7362; E-mail addresses: xclu@tsinghua.edu.cn*

[b] *National Engineering Research Center for Nanotechnology, Shanghai 200241, China*

1 S. J. Pearton, D. P. Norton, K. Ip, Y. W. Heo and T. Steiner, *Superlattices Microstruct.*, 2003, **34**, 3.

2 U. Ozgur, Y. I. Alivov, C. Liu, A. Teke, M. A. Reshchikov, S. Dogan, V. Avrutin, S. J. Cho and H. Morkoc, *J. Appl. Phys.*, 2005, **98**, 41301.
3 J. S. Zabinski, J. Corneille, S. V. Prasad, N. T. McDevitt and J. B. Bultman, *J. Mater. Sci.*, 1997, **32**, 5313.
4 S. V. Prasad and J. S. Zabinski, *Wear*, 1997, **203**, 498.
5 S. V. Prasad, S. D. Walck and J. S. Zabinski, *Thin Solid Films*, 2000, **360**, 107.
6 J. S. Zabinski, J. H. Sanders, J. Nainaparampil and S. V. Prasad, *Tribol. Lett.*, 2000, **8**, 103.
7 H. Mohseni and T. W. Scharf, *J. Vac. Sci. Technol. A*, 2012, **30**, 01A149.
8 H. Mohseni, B. A. Mensah, N. Gupta, S. G. Srinivasan and T. W. Scharf, *Tribol.Lubr. Technol.*, 2012, **68**, 17.
9 Z. M. Chai, X. C. Lu and D. N. He, *Surf. Coat. Technol.*, 2012, **207**, 361.
10 S. Y. Pung, K. L. Choy, X. Hou and C. X. Shan, *Nanotechnology*, 2008, **19**, 435609.
11 A. Wojcik, M. Godlewski, E. Guziewicz, R. Minikayev and W. Paszkowicz, *J. Cryst. Growth*, 2008, **310**, 284.
12 M. Leskela and M. Ritala, *Thin Solid Films*, 2002, **409**, 138.
13 M. Leskela and M. Ritala, *Angew. Chem. Int. Ed.*, 2003, **42**, 5548.
14 S. Jeon, S. Bang, S. Lee, S. Kwon, W. Jeong, H. Jeon, H. J. Chang and H. H. Park, *J. Electrochem. Soc.*, 2008, **155**, H738.
15 H. Makino, A. Miyake, T. Yamada, N. Yamamoto and T. Yamamoto, *Thin Solid Films*, 2009, **517**, 3138.
16 T. Krajewski, E. Guziewicz, M. Godlewski, L. Wachnicki, I. A. Kowalik, A. Wojcik-Glodowska, M. Lukasiewicz, K. Kopalko, V. Osinniy and M. Guziewicz, *Microelectron. J.*, 2009, **40**, 293.
17 N. Fujimura, T. Nishihara, S. Goto, J. F. Xu and T. Ito, *J. Cryst. Growth*, 1993, **130**, 269.
18 S. Park, C. S. Hwang, H. Y. Jeong, H. Y. Chu and K. I. Cho, *Electrochem. Solid-State Lett.*, 2008, **11**, H10.
19 M. H. Madsen, M. Aagesen, P. Krogstrup, C. Sorensen and J. Nygard, *Nanoscale Res. Lett.*, 2011, **6**, 516.
20 M. Xu, H. L. Lu, S. J. Ding, L. Sun, W. Zhang and L. K. Wang, *Chin. Phys. Lett.*, 2005, **22**, 2418.
21 B. Bhushan and A. V. Kulkarni, *Thin Solid Films*, 1996, **278**, 49.
22 Y. Qi and T. D. Mantei, *Surf. Coat. Technol.*, 2004, **177**, 394.
23 G. L. Doll, B. A. Mensah, H. Mohseni and T. W. Scharf, *J. Therm. Spray Techn.*, 2010, **19**, 510.
24 K. L. Johnson,In *Contact Mechanics*. Cambridge University Press, United Kingdom, 1987.